AVIATION
ISSN: 1648-7788 / eISSN: 1822-4180
2023 Volume 27 Issue 1: 36–46
https://doi.org/10.3846/aviation.2023.18461

A SIMULTANEOUS PATH PLANNING AND POSITIONING BASED ON ARTIFICIAL DISTRIBUTION OF LANDMARKS IN A GNSS DENIED ENVIRONMENT

Samaneh ELAHIAN, Mohammad-Ali AMIRI ATASHGAH *, Bahram TARVERDIZADEH

Faculty of New Sciences and Technologies, University of Tehran, Tehran, Iran

Received 3 March 2022; accepted 9 August 2022

Abstract. In recent years, exploration operations by autonomous robots are expanding into unknown environments on Earth, under the sea, or even on other planets. This paper proposes the idea of Concurrent Path Planning and Positioning (CPPAP) using artificially distributed landmarks, while no GNSS signal is available. The method encompasses an observability-based direction search algorithm for path planning in parallel with Simultaneous Localization and Mapping (SLAM) for localization. Most of the path planning methods utilize offline algorithms; however, the proposed method determines the robot's direction of motion in real-time, concurrently with the positioning tasks by the inclusion of the system observability, related to the features' distribution. Same as in all feature-based SLAMs, features play an important role in determination of the most observable direction, and hence the direction of the robot's motion. Moreover, the effectiveness of the distribution of the features and their pattern in the proposed method is investigated. To evaluate the efficiency and accuracy of the CPPAP, outcomes are compared with an existing random SLAM.

Keywords: concurrent path planning and positioning (CPPAP), simultaneous localization and mapping (SLAM), Eigenvalue observability analysis, artificial landmarks, GNSS denied environments.

Introduction

The necessity of operations in unknown environments or conditions where no signals of GNSS/GPS are available, motivates researchers to find heuristic/novel positioning and path planning methods; even without the necessity for external position fixing devices (Aminzadeh & Amiri Atashgah, 2018). However, any failure in navigation subsystems also may cause such circumstances. To perform- such missions, the implementation and utilization of a hybrid navigation and path planning methodis a must. Regarding the navigation tasks in unknown environments, Simultaneous Localization and Mapping (SLAM), has been an ever-growing method in recent years.

SLAM resources are mainly dedicated to the following subject matters; some articles concentrate on map accuracy by using different filters (Bahraini et al., 2018; F. Zhang et al., 2018; Y. Zhang et al., 2018). A number of them focus on SLAM consistency based on filter and observability analysis (Barrau & Bonnabel, 2015; G. Huang et al., 2008; G. P. Huang et al., 2009). Data association is another issue that is investigated by Leonard and Zoubir (2019), Yousif et al. (2015), G. Zhang et al. (2015).

Improvement of accuracy in SLAM by map enhancement is also of great interest. One of the methods for improving the accuracy of localization is system observability analysis. Many references deal with observability. Concerning the goal of this paper, these resources can be classified into three categories; The first class of works uses observability in miscellaneous applications to accurately define the parameters of the system model to gain more exact output results. Serpas et al. (2013) use observability criteria to determine the optimal position of the sensors for network optimization. In Lystianingrum et al. (2014) the observability analysis for battery temperature measurements is proposed by defining the optimal number of batteries and their position to decrease the cost. The authors in Van Den Berg et al. (2000) employ observability analysis to get the optimal position of tabular chemical reactor sensors. In another work, a different approach for observability and its condition is investigated

*Corresponding author. E-mail: *atashgah@ut.ac.ir*

for biochemical nonlinear systems (Aguilar-López et al., 2010). Regarding aerial and ground robots' navigation and state estimation, another category of observability-related research can be found in Bryson and Sukkarieh (2008), Huang et al. (2017), Batista et al. (2011), Hesch et al. (2013), Xu et al. (2020).

The next category of resources is dedicated to observability analysis for SLAM and navigation. In this type ofwork, observability is used for two purposes; some focus on essential conditions for SLAM observability and determination of the degree of observability in different environments. In L. Huang et al. (2017) employed the observability concept to determine the appropriate distribution of landmarks in the visual navigation system. Observability conditions and the effect of landmark arrangement on the observability of the system are considered in Chakraborty et al. (2017), Sharma et al. (2012), as well. The second class is articles that imply observability for real-time path planning in SLAM. In these articles, observability is used to define robot motion direction in unknown environments. Carlone et al. (2014) solve active path planning in SLAM by expected information from policy to select the best strategy for robot motion. Another approach for path planning in SLAM is coverage improvement that is implemented by the combination of model predictive control with the direction of robot motion to the desired location (Leung et al., 2006). A cognitive-based adaptive optimization algorithm for real-time active SLAM is also employed in Kalogeiton et al. (2019). They demonstrated that this algorithm has more robustness and efficiency in comparison with robot random movement. In the following, Sharma has used receding horizon control and information matrix to define the best path (Sharma, 2014); The path is planned in such a way that in each step, information achieved from sensors is increased. Moreover, Bryson and Sukkarieh (2008) are employing entropy as an information-based measurement to select the optimal trajectory for robot motion. In their research, observability is used as a decision rule to aid the path planning process.

Regarding path planning, which is of great interest in resources, Wen et al. (2020) improved path planning tasks in SLAM through dueling deep reinforcement learning algorithm. Path planning for exploring unknown environments is mainly implemented by A* and D* algorithms (Hasegawa & Fujimoto, 2016; Maurovic et al., 2018). Optimal path planning is another approach for optimization of mission time and traveled distance (Clemens et al., 2016; Fethi et al., 2018).

As priorly stated, this work is dedicated to concurrent path planning and navigation of an aerial robot's motion in real-time, based on observability analysis in an unknown environment with specific distribution of landmarks, so that an accurate map of the environment is achieved. The idea is such that, the aerial robot starts from an initial point and based on the pattern of landmarks, follows the generated path to reach a zone of interest. For this goal, the paper is organized as follows. In section 1 system development is described including positioning, observability, and path planning and then the proposed method is presented. In sections 2 and 3, simulations and results are presented and discussed. Finally, in the last section, conclusions are obtainable.

1. Theoretical framework

In the proposed method, it is assumed that an autonomous robot starts from an initial unknown point and moves along the path with the most observability to the destination while making an exact map of the environment. To perform this mission, the robot uses IMU and a camera to detect the landmarks. In each step, the task of estimating the robot and features position by an Extended Kalman filter (EKF-SLAM) is performed. The features are predetermined landmarks that the robot can recognize by image processing/data association algorithms from other landmarks that exist in the environment. These artificial features are arranged/distributed in the mission environment to guide the robot to the destination area. Hence, in this mission, the detection of features and their arrangement are very critical. Then, the goal is to determine the angle of robot motion in each step to guide the robot on a path that gives an accurate map of the outdoor environment. Accordingly, in this work, a novel method is proposed for concurrent real-time path planning and navigation using eigenvalues and eigenvectors of the observability Gramian via an EKF-SLAM; Hence, more observability in the path aids the filter to make a better estimation of the state variables. The proposed method can be used for real-time path planning in different applications such as ground and aerial vehicles, and also in marine (on Earth or other planets); wherein a robot starts from an initial unknown/known point and plans to arrive at a destination area for a specific task, service, or a self-rescue district (Figure 1).

In the following sections, basic concepts and assumptions in different aspects of the work are presented.

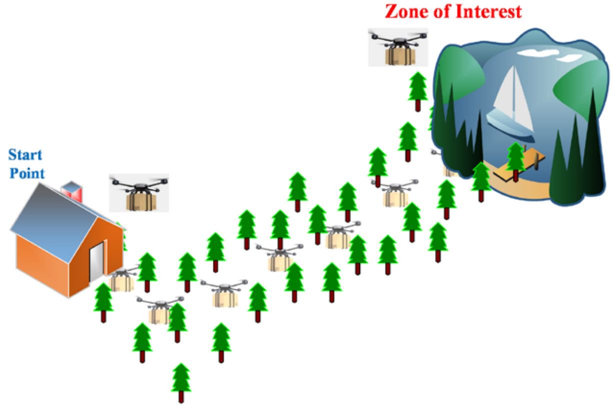

Figure 1. The CPPAP idea is to attain a zone of interest

1.1. Positioning

One of the positioning methods in a GNSS denied environment is visual-based navigation (Atashgah & Malaek, 2013). This method depends on how much the environment is known. The importance of this cognition is so much that it is used as a criterion for visual navigation methods classification. Myhre (2018) categorize these methods into non-priori (for an unknown environment) and priori methods (for a known environment). Non-priori methods are classified as mapless and SLAM methods. In this paper, SLAM is used for robot navigation in the environment.

One of the solutions for the SLAM problem is employing various types of filters. Different filters such as Kalman, particle, and information filters are proposed for SLAM, and most of them are based on the Bayes filter (Fraundorfer & Scaramuzza, 2012; Kurt-Yavuz & Yavuz, 2012; Bahraini et al., 2018). Kurt-Yavuz and Yavuz (2012) have compared different filters' performance in SLAM. They showed that the Root Mean Square Error (RMSE) for FastSLAM and UFastSLAM by 50 particles is approximately equal to EKF estimation. Correspondingly, UFastSLAM is known as the most efficient method with a Least Mean Square Error (LMSE) and the slowest one. In this manuscript, when SLAM is utilized for real-time operation, low complexity and delay in calculations are important. Accordingly, and due to the almost expected precision of the estimation, the EKF-SLAM is selected for the implementation of the proposed method.

EKF-SLAM

Measurement of all system states or direct measurement of some states is not practical because the system becomes more complex and expensive. Moreover, because of noise in sensor measurements and environmental disturbances, robot measurements during the time are not exact. Subsequently, using estimators to measure data indirectly or decrease measurement errors and increase the precision of the calculation is necessary. As mentioned above, in this work, direct measurement of position is not possible. So it should be calculated by velocity measurements which contain measurement noises. Therefore, EKF is used as a SLAM solution and includes two main steps; prediction and update. In prediction (Eq. (1) to Eq. (4)), state $\boldsymbol{x}$ and covariance $\boldsymbol{P}$ values are defined as follows:

$$\hat{\boldsymbol{X}}_{n+1}^{-} = \boldsymbol{F}\hat{\boldsymbol{X}}_{n}^{+} + \boldsymbol{w}_{n+1}; \quad (1)$$

$$\boldsymbol{Z}_{n+1} = \boldsymbol{H}_{k+1}\boldsymbol{X}_{n+1} + \boldsymbol{v}_{n+1}; \quad (2)$$

$$\boldsymbol{P}_{n+1}^{-} = \mathbf{F}_{n+1}\boldsymbol{P}_{n}^{+}\boldsymbol{F}_{n+1}{}^{T} + \boldsymbol{Q}; \quad (3)$$

$$\boldsymbol{K}_{n+1} = \boldsymbol{P}_{n+1}^{-}\boldsymbol{H}_{n+1}{}^{T}\left(\boldsymbol{H}_{n+1}\boldsymbol{P}_{n+1}^{-}\boldsymbol{H}_{n+1}{}^{T} + \mathbf{R}\right)^{-1}, \quad (4)$$

where $\boldsymbol{F}$ and $\boldsymbol{H}$ are Jacobian of motion and sensor measurement models, w_n and v_n are Gaussian processes and measurement noises with zero Mean and Q and R are noise covariances. Furthermore, the motion model is as follows:

$$\begin{bmatrix} x(n+1) \\ y(n+1) \\ \theta(n+1) \end{bmatrix} = \begin{bmatrix} x(n) \\ y(n) \\ \theta(n) \end{bmatrix} + \begin{bmatrix} \mathrm{V}\cdot dt\cdot\cos(\theta(n)) \\ \mathrm{V}\cdot dt\cdot\sin(\theta(n)) \\ \omega\cdot dt \end{bmatrix}. \quad (5)$$

In Eq. (5), θ, V, and ω represent the heading angle, total linear velocity in the xy plane, and vertical angular velocity, respectively. Accordingly, in the following, the state vector includes robot position and heading angle (a 3*1 matrix), and landmarks position in the field of view of the robot (Eq. (6)); n shows the number of landmarks seen by the robot at each step. The observation model includes the range and bearing angles of a landmark (Eq. (7)). Finally, the augmented state vector is defined as follows:

$$\mathbf{X}(\mathrm{k}) = \begin{bmatrix} Po(k) \\ \theta(k) \\ m_1(k) \\ m_2(k) \\ \vdots \\ m_n(k) \end{bmatrix}; \quad (6)$$

$$\boldsymbol{Z}_i(k) = \begin{bmatrix} \rho_i \\ \varphi_i \end{bmatrix} = \begin{bmatrix} \sqrt{(x_r - x_m)^2 + (y_r - y_m)^2} \\ tan^{-1}\left(\dfrac{y_r - y_m}{x_r - x_m}\right) - \theta \end{bmatrix}, \quad (7)$$

where Po, θ, and m_i indicate the vehicle position vector, heading angle, and the i^{th} landmark position vector, respectively. In the observation model, ρ_i and φ_i are range and bearing angle to the i^{th} landmark. In the following, the updated values of the state and covariance matrix are determined by Eq. (8) and Eq. (9), as follows:

$$\hat{\boldsymbol{X}}_{n+1}^{+} = \hat{\boldsymbol{X}}_{n+1}^{-} + \boldsymbol{K}_{n+1}\left(\boldsymbol{Z}_{n+1} - \boldsymbol{H}_{n+1}\hat{\boldsymbol{X}}_{n+1}^{-}\right); \quad (8)$$

$$\boldsymbol{P}_{n+1}^{+} = \left(\boldsymbol{I} - \boldsymbol{K}_{n+1}\boldsymbol{H}_{n+1}\right)\boldsymbol{P}_{n+1}^{-}\left(\boldsymbol{I} - \boldsymbol{K}_{n+1}\boldsymbol{H}_{n+1}\right)^{T} + \boldsymbol{K}_{n+1}\boldsymbol{R}\boldsymbol{K}_{n+1}^{T}. \quad (9)$$

1.2. Observability analysis

Observability analysis of the system exhibits that measurement of which output variables gives more precision for estimation of the input variables. More observability of the system means we can estimate the states more precisely; accordingly, in SLAM, if the robot moves in the direction with more observability, a better estimation of the state variables is gained. This is the main contribution of this work to the concurrent navigation and path planning of the robot. Concisely, the proposed method uses this rule to determine the robot path so that more accuracy in providing a map of the environment is gained.

Linear observability analysis

Different methods are proposed for linear systems (Eq. (10)) observability analysis. The two most common methods are the observability matrix and Gramian

(Eq. (11) and Eq. (12)). If the observability matrix is full rank, the system is observable. Likewise, if the Gramian matrix has a positive determinant, it is observable, and how much this determinant is greater, the degree of observability increases (Chen, 1999). The related mathematical equations are as follows:

$$\begin{aligned}\dot{\boldsymbol{X}} &= \boldsymbol{AX} + \boldsymbol{Bu} \\ \boldsymbol{Y} &= \boldsymbol{CX} + \boldsymbol{Du}\end{aligned}; \tag{10}$$

$$\mathbf{O} = \begin{bmatrix} \mathbf{C} \\ \mathbf{CA} \\ \mathbf{CA}^2 \\ \vdots \\ \mathbf{CA}^{\mathbf{n}-1} \end{bmatrix}; \tag{11}$$

$$\mathbf{W}_o\left(t_0 \cdot t_1\right) = \int_{t_0}^{t_1} \phi'(\tau \cdot t_0)\mathbf{C}'\left(\tau\right)\mathbf{C}\left(\tau\right)\phi\left(\tau \cdot t_0\right). \tag{12}$$

In which, $\boldsymbol{x}$ and $\boldsymbol{y}$ are state and output vectors, $\boldsymbol{u}$ is control input, $\mathbf{o}$ and $\mathbf{W}_o$ are observability and gram matrices and ϕ is the State Transition Matrix (STM).

Nonlinear observability analysis

The observability of a nonlinear system, compared to a linear one, is more challenging. Nevertheless, different approaches for nonlinear system observability analysis are proposed. There are two steps for system observability determination: selection of the matrix and proper criteria for interpretation of the degree of observability. Four matrices are proposed in the literature for nonlinear system observability, including observability (Nijmeijer & Schaft, 1990), gram (Lall et al., 2002) error covariance matrix (Hahn et al., 2003; Ham & Grover Brown, 1983), and Lie derivative matrix (Hermann et al., 1977). The full rank of the observability matrix (number of states equal to the rank of the matrix) shows the system is observable. This condition for observability Gramian has the same meaning. Rank condition only replies to observability by yes or no, but some conditions/criteria determine the degree of observability. Determinant, trace, condition number, singular values, and eigenvalues are criteria used for the assessment of the observability gained from the Gramian matrix (Eq. (13) to Eq. (15)).

$$\text{trace}\left(\mathbf{W}_o\right) = \sum_{i=1}^{n} \sigma_i\left(\mathbf{W}_o\right); \tag{13}$$

$$\text{CN} = \frac{\sigma_{\max}\left(\mathbf{W}_o\right)}{\sigma_{\min}\left(\mathbf{W}_o\right)}; \tag{14}$$

$$\text{NS}\left(\mathbf{W}_o\right) = \sigma_{\min}\left(\mathbf{W}_o\right), \tag{15}$$

where $\sigma_{\max}$ and $\sigma_{\min}$ are the maximum and minimum singular values of the observability Gramian. The More value of the determinants, eigenvalues, trace, and singular values conclude the larger observability and more accurate estimation. In contrast, the lower value of the condition number shows a greater degree of observability. The covariance matrix is used by different criteria such as eigenvalues (Ham et al., 1983) and observability rank (Hahn et al., 2003). Another method for the determination of nonlinear observability is the Lie derivative (Huang et al., 2017; Lee et al., 2006; Sharma et al., 2012; Butcher et al., 2017; Xu et al., 2020).

Among different criteria investigated for the system observability, eigenvalues and eigenvectors provide information about the degree and direction of observability. This direction has valuable information for SLAM path planning that helps the robot to move toward the direction in which its estimation is more exact than the other paths. More details of the method are described in the next parts.

1.3. Path planning

Path planning determines the path (x and y position) that the robot moves through it, to reach the goal. Different methods for path planning of autonomous robots are proposed in the literature. Each of them with a specific rule. Random methods such as A^* and D^* (Fu et al., 2018; Zammit & van Kampen, 2018), potential field method (Rasekhipour et al., 2017; Chen et al., 2014), and other methods based on sampling such as RRT and RRT* (Li et al., 2020; Zammit & van Kampen, 2018; Perez et al., 2012), roadmap (Wang & Cai, 2018; Niu et al., 2019) and heuristic methods (Qu et al., 2020; Bakdi et al., 2017; Fakoor et al., 2016) are some type of these methods.

González et al. (2016) reviewed different approaches for autonomous robot path planning and categorized them into four groups based on the graph search algorithms, sampling, interpolation, and numerical optimization (González et al., 2016). According to the results, the interpolation and graph search methods are extensively used compared to the other ones, due to their ability to produce an enhanced map of the environment and also fast and optimized implementation in real-time projects. In another work, Patle et al. (2019) surveyed strategies for mobile robot path planning and categorized them into classic, reactive (intelligent), and hybrid methods. Their research illustrates that, even though reactive methods are more robust in an uncertain environment and have better performance for real-time projects, they are not proper choices for low-cost robots; because of the long time and high cost of calculations.

Among classic methods, the potential field method compromises more utilization which usually is used offline. In this method, goals and obstacles are modeled as attractive and repellent fields, where the robot moves away from obstacles as far as possible and tends toward the goal. In all of those methods, the main goal is finding the shortest path from a start point to the end while avoiding obstacles. Mac et al. (2016) presented the strengths and drawbacks of heuristic methods such as fuzzy, neuro-fuzzy, genetic algorithm, and particle swarm optimization. Aggarwal and Kumar (2020) had a different approach and categorized these methods into three groups concluding representative, cooperative and non-cooperative, and compared them from different points of view such as path length, cost, time and energy efficiency, robustness, and collision avoidance. Subjects matter in SLAM, the accuracy of the estimation and preparing an exact map of the environment is very important. Hence, developing a new method of real-time path planning is an essential task in the area.

All of the above-mentioned methods try to find the optimal path from the start point to the end goal while avoiding the obstacles in a graphed environment. This article proposes a different approach for autonomous robot path planning; starting from an initial known/unknown point and heading to a destination area than a target point. Therefore, employing a real-time path planning method is a must. According to the reviewed path planning methods (in the introduction section), only a few methods are appropriate for this aim.

The Proposed CPPAP

For 2D path planning, while the flight altitude is attained constant, the information of the robot velocity and heading suffice. According to the observability analysis, when a system comprises more degree of observability, the state vector can be predicted more accurately by measuring the outputs and observations. As stated before, the main idea of the proposed method is finding a heading angle so that the robot moves in the direction that system observability becomes maximum and therefore an accurate map of the environment is achieved.

To achieve the defined goal, a new method based on eigenvectors of the observability Gramian is proposed. By calculation of the observability matrix (gained from Eq. (11)), the Gramian matrix with a decent approximation is attained by Eq. (16).

$$\mathbf{W}_o = \mathbf{O}^T \mathbf{O}. \quad (16)$$

In this equation, O is the observability matrix and is calculated by Eq. (11). Regarding the calculation of the observability matrix, the coefficient matrices, **A** and **C**, which are Jacobians of the motion and observation models are determined as below.

$$\boldsymbol{A} = \begin{bmatrix} \\ 1\,0 & -v\sin(\theta + w\cdot dt) & 0\,0 \\ 0\,1 & -v\cos(\theta + w\cdot dt) & 0\,0 \\ 0\,0 & 1 & 0\,0 \\ 0\,0 & 0 & 1\,0 \\ 0\,0 & 0 & 0\,1 \end{bmatrix}; \quad (17)$$

$$\boldsymbol{C} = \frac{1}{q}\cdot\begin{bmatrix} -\delta_x\sqrt{q} & -\delta_y\sqrt{q} & 0 & \delta_x\sqrt{q} & \delta_y\sqrt{q} \\ \delta_y & -\delta_x & -q & -\delta_y & \delta_x \end{bmatrix}, \quad (18)$$

where *v*, *w*, and θ the linear and angular velocity and the robot direction angle; and *q*, δ_x, and δ_y as squares of the distance from the robot to a landmark and distance in the x and y-direction, respectively. In each step of the motion, the observability degree for all landmarks is achieved by determining eigenvalues. The eigenvector of the found biggest eigenvalue shows the most observable direction in each step (Eq. (19) and Eq. (20)). Supposing at time t_i, *n* landmarks are in robot's view:

$$\lambda_{ti-\max} = \max\left(\lambda_{ti-1} \ldots \lambda_{ti-n}\right); \quad (19)$$

$$v_{ti-\max} = v_{ti}\left(\lambda_{ti-\max}\right) = \begin{bmatrix} v_{mx} \\ v_{my} \end{bmatrix}. \quad (20)$$

$$\theta_{obs} = \arctan\left(\frac{V_{my}}{V_{mx}}\right). \quad (21)$$

So the rotation angle is defined as

$$\Delta\theta_{rot} = \theta_{robot} - \theta_{eigen}. \quad (22)$$

As path planning and EKF-SLAM both are based on feature identification, any problem with it, causes the robot to go to an unknown goal. In the implementation of CPPAP, it's supposed that the robot can't move backward and the rotation angle is restricted between ±90 degrees. The proposed method is thoroughly described in Table 1 and Figure 2, respectively.

Table 1. Algorithm of the proposed CPPAP (Algorithm 1)

Mission Starts
EKF-SLAM Starts
Path-Planning Starts
Make Observability dataset
Fori=1:numLmk **do**
Calculate observability matrix (O) according to Eq. (13).
Calculate observability Gramian (W_o) by Eq. (18)
Determine max eigenvalue of W_0
End
Search the most observable direction
Find the max eigenvalue of all eigenvalues in each step
Select the eigenvector of the max eigenvalue
$\theta_{rot} = \theta_{MOD} - \theta_{rob}$ (MOD: most observable direction)
Perform Remaining EKF-SLAM Tasks
Path-Planning Ends
EKF-SLAM Ends
Mission Decision Making Tasks
Mission Ends

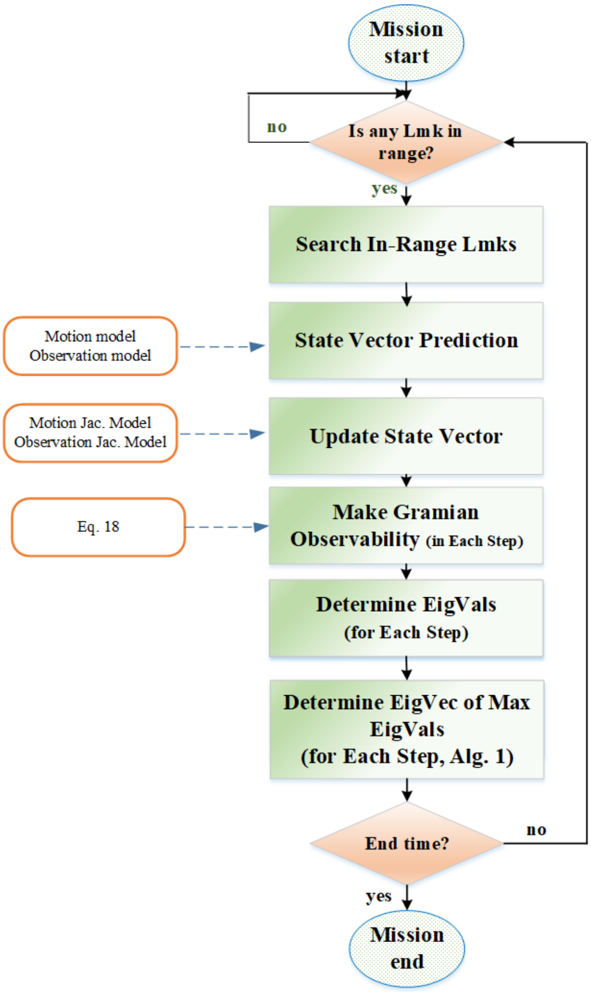

Figure 2. Block diagram of the proposed CPPAP

2. Simulations and results

Simulations have two goals; the first aim is performance evaluation of the proposed method by comparing it with an existing random SLAM, in the same environment with a similar distribution of the landmarks. Another goal is an investigation into the effect of feature distribution/pattern in the environment on system observability. To this end, two types of landmark distributions, such as triangular and wave-like forms, with approximately 120 features are adopted. It should be noted that each feature is placed at an approximately identical distance from its neighbors in all distribution patterns so that identical conditions for efficiency analysis of the methods are prepared. Moreover, to have a decent performance evaluation, the implemented EKF-SLAM results are compared with the true (error-free) path and dead reckoning predictions (Figures 3 and 4).

In the following, Table 2 contains the simulation parameters' values and conditions. Furthermore, to have an identical metric for comparing the efficiency of the methods in simulations, the initial state of the robot and covariance matrix is assumed as, [–10 –20 0] and $I_{3\times3}$, respectively.

Table 2. Simulation conditions

Parameter	Value	Unit
Max. Robot View Range	85	m
Cov. Matrix Initial Value	$I_{3\times3}$	–
Range Noise Std	0.5	m
Bearing Noise Std	0.573	degree

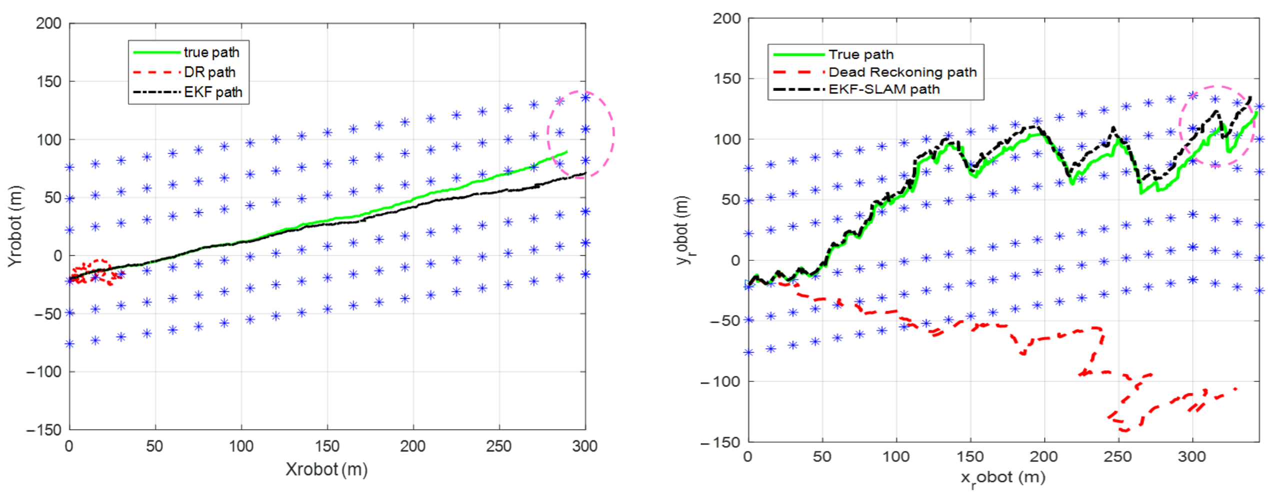

(a) Random SLAM

(b) CPPAP

Figure 3. Simulation results for a triangular pattern of landmarks

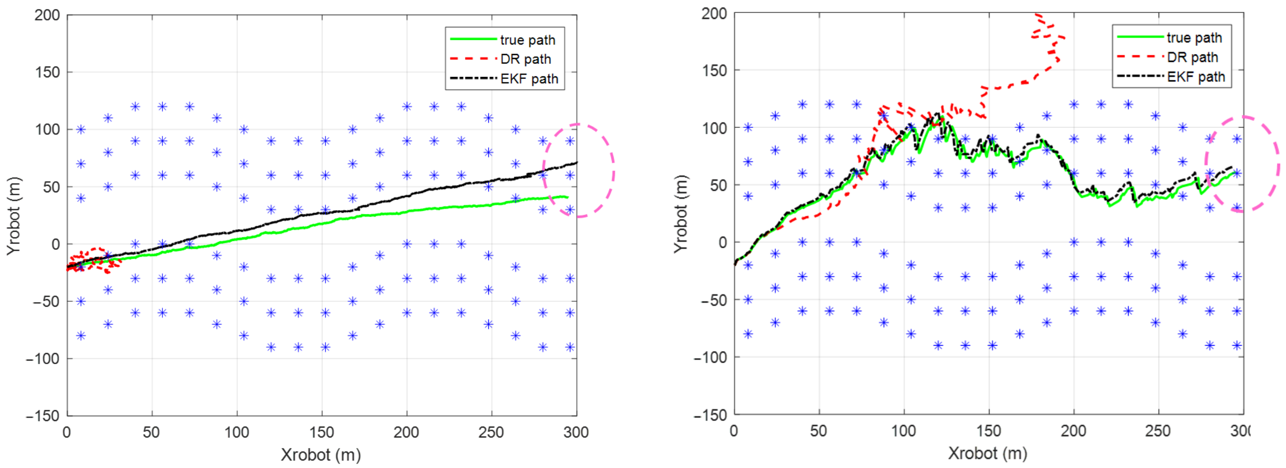

(a) Random SLAM (b) CPPAP

Figure 4. Simulation results for a sinusoidal/wave-like pattern of landmarks

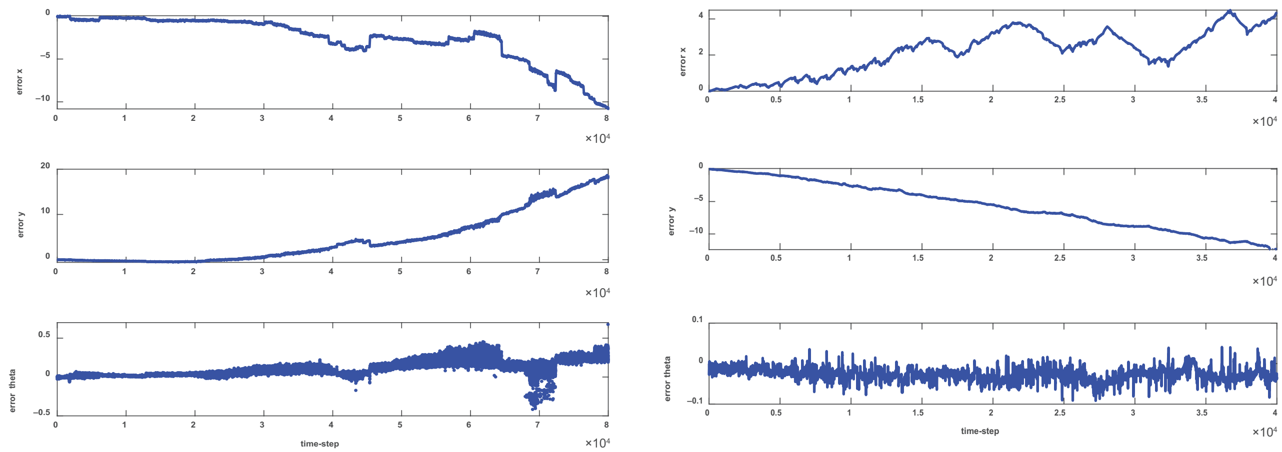

(a) Random SLAM (b) CPPAP

Figure 5. Performance evaluation for a triangular pattern of landmarks

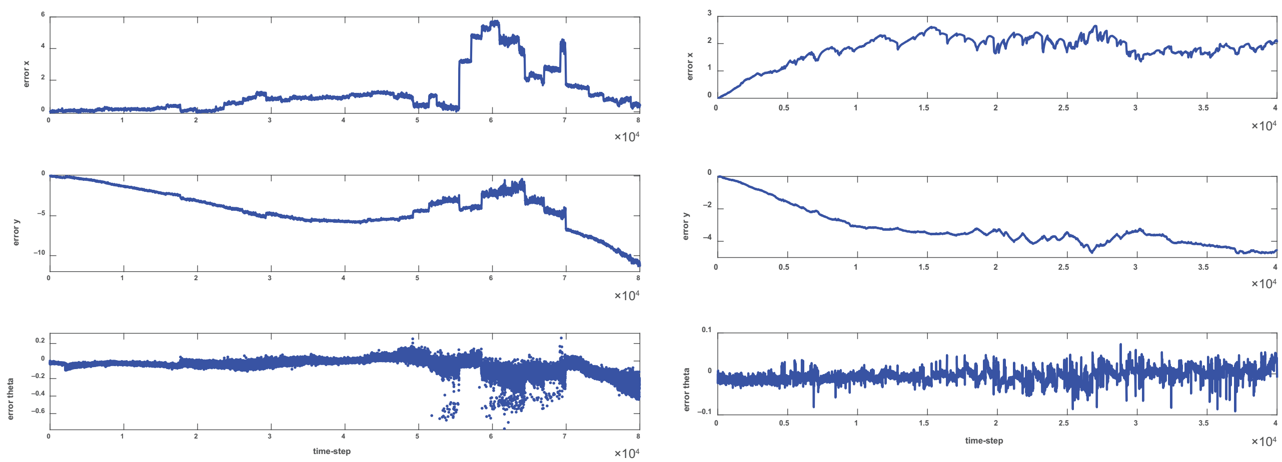

(a) Random SLAM (b) CPPAP

Figure 6. Performance evaluation for a sinusoidal/wave-like pattern of landmarks

To simulate the outdoor environment, wide variations in the *x*- and *y*- directions are considered for the robot's motion. In both scenarios, robot motion starts at position [0, 0], and the goal is an area that is fixed on the x component at 300 and is variable in the y-direction. The y component in CPPAP is determined by the observability value at that step. Simulations are conducted for 800 seconds by a 0.02-second time step.

In the following, errors in the robot's x, and y position directions, and heading angle, for both scenarios (triangular and sinusoidal/wave-like patterns) and both path planning methods (random SLAM and the CPPAP) are demonstrated in Figures 5 and 6.

3. Discussions

The main goal of a path planning method, based on observability, is improvement of the accuracy of the features' localization in the mapping process. Consequently, to compare the accuracy of the EKF-SLAM in both path planning methods and both scenarios, the covariance matrix of the EKF-SLAM (Tao et al., 2007) is used. Therefore, in each step of the simulation, the trace of the covariance matrix is calculated; The accumulated error values demonstrate the accuracy along the whole path. This value is used as a criterion for map accuracy assessment. Figure 3 shows the path that robot moves from the start point to the destination area by both random SLAM and CPPAP methods for triangular distribution. Subsequently, Figure 4 exhibits the results for a wave-like landmark distribution. As is seen in Figures 3 and 4, by the employment of the CPPAP method, the robot moves in the environment merely exploiting features guidance to the goal destination area while realizing more new features with more observability in the path. In path planning with this algorithm, the robot moves toward the new unknown features which are away from it. On the other hand, the robot moves within the borders which is determined by the placement of the features; Where in the sections attempt to decrease the uncertainties in the mapping process.

To have an estimation of error in the EKF-SLAM-based path, RMSE of robot position (in x and y directions) is calculated, as well. Trace of the covariance matrix shows the overall mean square error. Therefore, the accuracy of the two methods is compared by the utilization of the trace of the covariance matrix and RMSE. According to the results displayed in Table 3, the trace of the covariance in the CPPAP method is less than the random SLAM, in both feature distributions. Similarly, the proposed method has less RMSE that confirms the outcomes from the trace of covariance. Moreover, the CPPAP is faster than the random method.

Comparison between two distributions shows that wave-like distribution gains more observability in the path and leads to more accurate path planning. Also, RMSE in the triangular distribution has an increasing trend for both methods while this trend for the sinusoidal pattern increases at the beginning and continues uniformly. The error trend especially in a triangular pattern has similar behavior to robot movement due to the number of visited/seen landmarks in the robot's field of view.

Another outcome is that the average number of seen features in the robot path for wave-like and triangular distributions is 32.9 and 42.2, respectively. Because the landmarks/features are the basis of the CPPAP method, the number of seen features in each step affects the efficiency of the planned path, as well. As is shown in Figure 7, in random methods the number of seen landmarks exhibits a smooth trend while in the CPPAP method it shows a fluctuating trend. Accordingly, it can be concluded that more features in the robot field of view necessarily don't lead to more accurate mapping.

As Table 3 demonstrates, path planning by the random method desires more time than the proposed CPPAP method. Since in the random path planning method the robot moves randomly in different directions with a small amount of deviation, the time to reach to destination area is more than the time needed for the CPPAP method. Consequently, the proposed method takes more time to perform the mission relative to the random method.

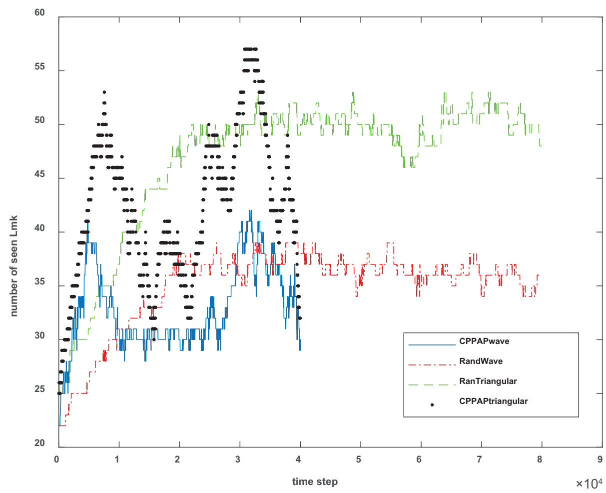

Figure 7. Number of visited landmarks for all conditions

Table 3. Performance evaluation outcomes

Pattern Type	Triangular	Triangular	Wave-like	Wave-like
Path planning method	CPPAP	Random	CPPAP	Random
Trace of Covariance	3.46	7.66	2.71	5.88
Time to reach the goal (s)	700	1876	590	1889
Path RMSE (x and y error)	2.4	4.06	0.84	1.89

Conclusions

Using the proposed method, the observability of the system increases and precise estimation of the robot and landmarks' position in a feature-based SLAM is enhanced. Besides, simulation experiments of EKF-SLAM path planning for two different geometries of the artificially distributed landmarks were conducted by the Gramian covariance and random SLAM methods. Results indicated that the map achieved by observability-based path planning is more accurate and more computationally efficient than the random-based SLAM one. It is worth noting that by using the proposed approach and with the desired distribution of the landmarks, some kind of obstacle avoidance also can be conducted. Moreover, this type of obstacle avoidance method can be a research area for future works. To enrich the proposed activity, the following topics can be put on the agenda: (a) SITL/HITL implementation and evaluations of the idea, (b) development of the work in a multi-agent environment, and lastly (c), the inclusion of obstacles and dynamic landmarks to the scenes and evaluation of the idea for collision avoidance tasks.

References

Aguilar-López, R., Mata-Machuca, J. L., & Martinez-Guerra, R. (2010). On the observability for a class of nonlinear (bio) chemical systems. *International Journal of Chemical Reactor Engineering, 8*(1). https://doi.org/10.2202/1542-6580.2052

Aggarwal, S., & Kumar, N. (2020). Path planning techniques for unmanned aerial vehicles: A review, solutions, and challenges. *Computer Communications, 149*, 270–299. https://doi.org/10.1016/j.comcom.2019.10.014

Aminzadeh, A., & Amiri Atashgah, M. A. (2018). Feature article: Implementation and performance evaluation of optical flow navigation system under specific conditions for a flying robot. *IEEE Aerospace and Electronic Systems Magazine, 33*(11), 20–28. https://doi.org/10.1109/MAES.2018.170075

Amiri Atashgah, M. A., & Malaek, S. M. B. (2013). Prediction of aerial-image motion blurs due to the flying vehicle dynamics and camera characteristics in a virtual environment. *Proceedings of the Institution of Mechanical Engineers, Part G: Journal of Aerospace Engineering, 227*(7), 1055–1067. https://doi.org/10.1177/0954410012450107

Bahraini, M. S., Bozorg, M., & Rad, A. B. (2018). A new adaptive UKF algorithm to improve the accuracy of SLAM. *International Journal of Robotics, 5*(1), 35–46.

Bakdi, A., Hentout, A., Boutami, H., Maoudj, A., Hachour, O., & Bouzouia, B. (2017). Optimal path planning and execution for mobile robots using genetic algorithm and adaptive fuzzy-logic control. *Robotics and Autonomous Systems, 89*, 95–109. https://doi.org/10.1016/j.robot.2016.12.008

Barrau, A., & Bonnabel, S. (2015). *An EKF-SLAM algorithm with consistency properties*. Cornell University. http://arxiv.org/abs/1510.06263

Batista, P., Silvestre, C., & Oliveira, P. (2011). Single range aided navigation and source localization: Observability and filter design. *Systems & Control Letters, 60*(8), 665–673. https://doi.org/10.1016/j.sysconle.2011.05.004

Bryson, M., & Sukkarieh, S. (2008). Observability analysis and active control for airborne SLAM. *IEEE Transactions on Aerospace and Electronic Systems, 44*(1), 261–280. https://doi.org/10.1109/TAES.2008.4517003

Butcher, E. A., Wang, J., & Lovell, T. A. (2017). On Kalman filtering and observability in nonlinear sequential relative orbit estimation. *Journal of Guidance, Control, and Dynamics, 40*(9), 2167–2182. https://doi.org/10.2514/1.G002702

Carlone, L., Du, J., Kaouk Ng, M., Bona, B., & Indri, M. (2014). Active SLAM and exploration with particle filters using Kullback-Leibler divergence. *Journal of Intelligent and Robotic Systems: Theory and Applications, 75*(2), 291–311. https://doi.org/10.1007/s10846-013-9981-9

Chakraborty, A., Misra, S., Sharma, R., & Taylor, C. N. (2017). Observability conditions for switching sensing topology for cooperative localization. *Unmanned Systems, 5*(3), 141–157. https://doi.org/10.1142/S2301385017400039

Chen, C. (1999). *Linear system theory and design*. Oxford University Press.

Chen, Y. B., Luo, G. C., Mei, Y. S., Yu, J. Q., & Su, X. L. (2014). UAV path planning using artificial potential field method updated by optimal control theory. *International Journal of Systems Science, 47*(6), 1407–1420. https://doi.org/10.1080/00207721.2014.929191

Clemens, J., Reineking, T., & Kluth, T. (2016). An evidential approach to SLAM, path planning, and active exploration. *International Journal of Approximate Reasoning, 73*, 1–26. https://doi.org/10.1016/j.ijar.2016.02.003

Fakoor, M., Kosari, A., & Jafarzadeh, M. (2016). Humanoid robot path planning with fuzzy Markov decision processes. *Journal of Applied Research and Technology, 14*(5), 300–310. https://doi.org/10.1016/j.jart.2016.06.006

Fethi, D., Nemra, A., Louadj, K., & Hamerlain, M. (2018). Simultaneous localization, mapping, and path planning for unmanned vehicle using optimal control. *Advances in Mechanical Engineering, 10*(1). https://doi.org/10.1177/1687814017736653

Fraundorfer, F., & Scaramuzza, D. (2012). Visual odometry: Matching, robustness, optimization, and applications. *IEEE Robotics & Automation Magazine*, *19*(2). https://doi.org/10.1109/MRA.2012.2182810

Fu, B., Chen, L., Zhou, Y., Zheng, D., Wei, Z., Dai, J., & Pan, H. (2018). An improved A* algorithm for the industrial robot path planning with high success rate and short length. *Robotics and Autonomous Systems, 106*, 26–37. https://doi.org/10.1016/j.robot.2018.04.007

González, D., Pérez, J., Milanés, V., & Nashashibi, F. (2016). A review of motion planning techniques for automated vehicles. *IEEE Transactions on Intelligent Transportation Systems, 17*(4), 1135–1145. https://doi.org/10.1109/TITS.2015.2498841

Hahn, J., Edgar, T. F., Marquardt, W. (2003). Controllability and observability covariance matrices for the analysis and order reduction of stable nonlinear systems. *Journal of Process Control, 13*(2), 115–127. https://doi.org/10.1016/S0959-1524(02)00024-0

Ham, F. M., & Grover Brown, R. (1983). Observability, eigenvalues, and Kalman filtering. *IEEE Transactions on Aerospace and Electronic Systems, AES-19*(2), 269–273. https://doi.org/10.1109/TAES.1983.309446

Hasegawa, Y., & Fujimoto, Y. (2016). Experimental verification of path planning with SLAM. *IEEJ Journal of Industry Applications, 5*(3), 253–260. https://doi.org/10.1541/ieejjia.5.253

Hermann, R., Krener, A. (1977). Nonlinear controllability and observability. *IEEE Transactions on Automatic Control, AC-22*(5), 728–740. https://doi.org/10.1109/TAC.1977.1101601

Hesch, J. A., Kottas, D. G., Bowman, S. L., & Roumeliotis, S. I. (2013). Camera-IMU-based localization: Observability analysis and consistency improvement. *The International Journal of Robotics Research, 33*(1), 182–201. https://doi.org/10.1177/0278364913509675

Huang, G. P., Mourikis, A. I., Roumeliotis, S. I. (2008). Analysis and improvement of the consistency of extended Kalman filter based SLAM. In *IEEE International Conference on Robotics and Automation (ICRA)*. IEEE Xplore. https://doi.org/10.1109/ROBOT.2008.4543252

Huang, G. P., Mourikis, A. I., & Roumeliotis, S. I. (2009). On the complexity and consistency of UKF-based SLAM. In *2009 IEEE International Conference on Robotics and Automation*. IEEE. https://doi.org/10.1109/ROBOT.2009.5152793

Huang, L., Song, J., Zhang, Ch. (2017). Observability analysis and filter design for a vision inertial absolute navigation system for UAV using landmarks. *Optik, 149*, 455–468. https://doi.org/10.1016/j.ijleo.2017.09.060

Kalogeiton, V. S., Ioannidis, K., Sirakoulis, G. C., & Kosmatopoulos, E. B. (2019). Real-time active SLAM and obstacle avoidance for an autonomous robot based on stereo vision. *Cybernetics and Systems, 50*(3), 239–260. https://doi.org/10.1080/01969722.2018.1541599

Kurt-Yavuz, Z., & Yavuz, S. (2012). A comparison of EKF, UKF, FastSLAM2.0, and UKF-based FastSLAM algorithms. In *2012 IEEE 16th International Conference on Intelligent Engineering Systems (INES)* (pp. 37–43). IEEE. https://doi.org/10.1109/INES.2012.6249866

Lall, S., Marsden, J. E., & Glavaški, S. (2002). A subspace approach to balanced truncation for model reduction of nonlinear control systems. *International Journal of Robust and Nonlinear Control, 12*(6), 519–535. https://doi.org/10.1002/rnc.657

Lee, K. W., Wijesoma, W. S., Ibanez Guzman, J. (2006). On the observability and observability analysis of SLAM. In *2006 IEEE/RSJ International Conference on Intelligent Robots and Systems*. IEEE. https://doi.org/10.1109/IROS.2006.281646

Leonard, M. R., & Zoubir, A. M. (2019). Multi-Target tracking in distributed sensor networks using particle PHD filters. *Signal Processing, 159*, 130–146. https://doi.org/10.1016/j.sigpro.2019.01.020

Leung, C., Huang, S., & Dissanayake, G. (2006). Active SLAM using model predictive control and attractor based exploration. In *IEEE International Conference on Intelligent Robots and Systems* (pp. 5026–5031). IEEE. https://doi.org/10.1109/IROS.2006.282530

Lystianingrum, V., Hredzak, B., Agelidis, V. G., & Djanali, V. S. (2014). Observability degree criteria evaluation for temperature observability in a battery string towards optimal thermal sensors placement. In *2014 IEEE 9th International Conference on Intelligent Sensors, Sensor Networks and Information Processing (ISSNIP)*. IEEE. https://doi.org/10.1109/ISSNIP.2014.6827641

Mac, T. T., Copot, C., Tran, D. T., & De Keyser, R. (2016). Heuristic approaches in robot path planning: A survey. *Robotics and Autonomous Systems, 86*, 13–28. https://doi.org/10.1016/j.robot.2016.08.001

Maurovic, I., Seder, M., Lenac, K., & Petrovic, I. (2018). Path planning for active SLAM based on the D*algorithm with negative edge weights. *IEEE Transactions on Systems, Man, and Cybernetics: Systems, 48*(8), 1321–1331. https://doi.org/10.1109/TSMC.2017.2668603

Myhre, N. (2018). *Vision-aided navigation using tracked landmarks* [Doctoral Dissertations and Master's Theses]. Embry-Riddle Aeronautical University. https://commons.erau.edu/edt/390

Nijmeijer, H., & van der Schaft, A. (1990). *Nonlinear dynamical control systems*. Springer. https://doi.org/10.1007/978-1-4757-2101-0

Niu, H., Savvaris, A., Tsourdos, A., & Ji, Z. (2019). Voronoi-visibility roadmap-based path planning algorithm for unmanned surface vehicles. *The Journal of Navigation, 72*(4), 850–874. https://doi.org/10.1017/S0373463318001005

Patle, B. K., Babu L, G., Pandey, A., Parhi, D. R. K., & Jagadeesh, A. (2019). A review: On path planning strategies for navigation of mobile robot. *Defence Technology, 15*(4), 582–606. https://doi.org/10.1016/j.dt.2019.04.011

Perez, A., Platt, R., Konidaris, G., Kaelbling, L., & Lozano-Perez, T. (2012). LQR-RRT*: Optimal sampling-based motion planning with automatically derived extension heuristics. In *IEEE International Conference on Robotics and Automation* (pp. 2537–2542). IEEE. https://doi.org/10.1109/ICRA.2012.6225177

Qu, C., Gai, W., Zhong, M., & Zhang, J. (2020). A novel reinforcement learning based grey wolf optimizer algorithm for unmanned aerial vehicles (UAVs) path planning. *Applied Soft Computing, 89*, 106099. https://doi.org/10.1016/j.asoc.2020.106099

Rasekhipour, Y., Khajepour, A., Chen, S. K., & Litkouhi, B. (2017). A potential field-based model predictive path-planning controller for autonomous road vehicles. *IEEE Transactions on Intelligent Transportation Systems, 18*(5), 1255–1267. https://doi.org/10.1109/TITS.2016.2604240

Serpas, M., Hackebeil, G., Laird, C., & Hahn, J. (2013). Sensor location for nonlinear dynamic systems via observability analysis and MAX-DET optimization. *Computers and Chemical Engineering, 48*, 105–112. https://doi.org/10.1016/j.compchemeng.2012.07.014

Sharma, R. (2014). Observability based control for cooperative localization. In *2014 International Conference on Unmanned Aircraft Systems (ICUAS)* (pp. 134–139). IEEE. https://doi.org/10.1109/ICUAS.2014.6842248

Sharma, R., Beard, R. W., Taylor, C. N., & Quebe, S. (2012). Graph-based observability analysis of bearing-only cooperative localization. *IEEE Transactions on Robotics, 28*(2), 522–529. https://doi.org/10.1109/TRO.2011.2172699

Tao, T., Huang, Y., Sun, F., Wang, T. (2007). Motion planning for SLAM based on frontier exploration. In *2007 International Conference on Mechatronics and Automation*. IEEE. https://doi.org/10.1109/ICMA.2007.4303879

Van Den Berg, F. W. J., Hoefsloot, H. C. J., Boelens, H. F. M., & Smilde, A. K. (2000). Selection of optimal sensor position in a tubular reactor using robust degree of observability criteria. *Chemical Engineering Science, 55*(4), 827–837. https://doi.org/10.1016/S0009-2509(99)00360-7

Wang, Z., & Cai, J. (2018). Probabilistic roadmap method for path-planning in radioactive environment of nuclear facilities. *Progress in Nuclear Energy, 109*, 113–120. https://doi.org/10.1016/j.pnucene.2018.08.006

Xu, W., He, D., Cai, Y., & Zhang, F. (2022). Robots' state estimation and observability analysis based on statistical motion models. *IEEE Transactions on Control Systems Technology, 30*(5), 2030–2045. https://doi.org/10.1109/TCST.2021.3133080

Yousif, K., Bab-Hadiashar, A., & Hoseinnezhad, R. (2015). An overview to visual odometry and visual SLAM: Applications to mobile robotics. *Intelligent Industrial Systems, 1*(4), 289–311. https://doi.org/10.1007/s40903-015-0032-7

Zammit, C., & van Kampen, E. J. (2018). Comparison between A* and RRT algorithms for UAV path planning. In *2018 AIAA Guidance, Navigation, and Control Conference, 2018*, 210039. Aerospace Research Central. https://doi.org/10.2514/6.2018-1846

Zhang, F., Li, S., Yuan, S., Sun, E., & Zhao, L. (2018). Algorithms analysis of mobile robot SLAM based on Kalman and particle filter. In *2017 9th International Conference On Modelling, Identification and Control (ICMIC)* (pp. 1050–1055). IEEE. https://doi.org/10.1109/ICMIC.2017.8321612

Zhang, G., & Vela, P. A. (2015). Good features to track for visual SLAM. In *Proceedings of the IEEE Computer Society Conference on Computer Vision and Pattern Recognition* (pp. 1373–1382). IEEE. https://doi.org/10.1109/CVPR.2015.7298743

Zhang, Y., Zhang, T., & Huang, S. (2018). Comparison of EKF based SLAM and optimization based SLAM algorithms. In *2018 13th IEEE Conference on Industrial Electronics and Applications (ICIEA)* (pp. 1308–1313). https://doi.org/10.1109/ICIEA.2018.8397911

Notations

F – Jacobian of robot motion model;
H – Jacobian of sensor model;
K – Kalman gain;
m(k) – landmarks position;
O – observability matrix;
P(k) – robot position;
Q – Covariance of the process noise;
R – Covariance of the measurement noise;
$\mathbf{v}_n$ – measurement noise;
$\mathbf{w}_n$ – process noise;
$\mathbf{W_o}$ – Gramian;
X – state matrix;
Z – observation matrix;
Θ(k) – robot heading angle;
σ_{min} – minimum singular value;
σ_{max} – maximum singular value;
$\boldsymbol{\phi}(t)$ – state transition matrix.

Abbreviations

CN – Condition Number;
CPPAP – Concurrent Path Planning and Positioning;
EKF – Extended Kalman Filter;
GNSS – Global Navigation Satellite Systems;
LMSE – Least Mean Square Error;
NS – near singularity;
RMSE – Root Mean Square Error;
SLAM – Simultaneously Localization and Mapping;
STM – State Transition Matrix;
Std – Standard Deviation.